High vapour pressure deficit enhances turgor limitation of stem growth in an Asian tropical rainforest tree

Peters, Richard L.; Kaewmano, Arisa; Fu, Pei Li; Fan, Ze Xin; Sterck, Frank et al

ORIGINAL ARTICLE

High vapour pressure deficit enhances turgor limitation of stem growth in an Asian tropical rainforest tree

Richard L. Peters[1,2] | Arisa Kaewmano[3,4] | Pei-Li Fu[3,5] | Ze-Xin Fan[3,5] | Frank Sterck[6] | Kathy Steppe[2] | Pieter A. Zuidema[6]

[1]Department of Environmental Sciences—Botany, University of Basel, Basel, Switzerland

[2]Laboratory of Plant Ecology, Department of Plants and Crops, Faculty of Bioscience Engineering, Ghent University, Ghent, Belgium

[3]CAS Key Laboratory of Tropical Forest Ecology, Xishuangbanna Tropical Botanical Garden, Chinese Academy of Sciences, Mengla, Yunnan, China

[4]University of the Chinese Academy of Sciences, Beijing, China

[5]Ailaoshan Station of Subtropical Forest Ecosystem Studies, Xishuangbanna Tropical Botanical Garden, Chinese Academy of Sciences, Jingdong, Yunnan, China

[6]Forest Ecology & Forest Management Group, Wageningen University, Wageningen, The Netherlands

Correspondence
Ze-Xin Fan, CAS Key Laboratory of Tropical Forest Ecology, Xishuangbanna Tropical Botanical Garden, Chinese Academy of Sciences, Mengla, Yunnan 666303, China.
Email: fanzexin@xtbg.org.cn

Funding information
Swiss National Science Foundation, Grant/Award Number: P2BSP3_184475; National Natural Science Foundation of China, Grant/Award Numbers: 3186113307, 31870591

Abstract

Tropical forests are experiencing increases in vapour pressure deficit (D), with possible negative impacts on tree growth. Tree-growth reduction due to rising D is commonly attributed to carbon limitation, thus overlooking the potentially important mechanism of D-induced impairment of wood formation due to an increase in turgor limitation. Here we calibrate a mechanistic tree-growth model to simulate turgor limitation of radial stem growth in mature *Toona cilitata* trees in an Asian tropical forest. Hourly sap flow and dendrometer measurements were collected to simulate turgor-driven growth during the growing season. Simulated seasonal patterns of radial stem growth matched well with growth observations. Growth mainly occurred at night and its pre-dawn build-up appeared to be limited under higher D. Across seasons, the night-time turgor pressure required for growth was negatively related to previous midday D, possibly due to a relatively high canopy conductance at high D, relative to stem rehydration. These findings provide the first evidence that tropical trees grow at night and that turgor pressure limits tree growth. We suggest including turgor limitation of tree stem growth in models also for tropical forest carbon dynamics, in particular, if these models simulate effects of warming and increased frequency of droughts.

KEYWORDS
leaf water potential, point dendrometer, sap flow, tree growth, tropical rainforest, turgor-driven growth modelling

1 | INTRODUCTION

Understanding the impact of changing environmental conditions on tree growth and its variability is critical for more accurately constraining global carbon cycle dynamics (Bonan, 2008; Friedlingstein et al., 2019; Nemani et al., 2003; Pan et al., 2011). However, the mechanisms by which climatic variability drives tree growth are poorly understood. For instance, current vegetation models cannot explain empirical observations of tree growth variability (Fatichi et al., 2019; Klesse et al., 2018). These vegetation

models apply the source-limited growth hypothesis, which assumes that growth is a function of only carbon assimilation in the tree crown, which then dictates tree growth variability (Fatichi et al., 2014; Friend et al., 2019). New empirical evidence indeed points towards the important role of 'sink' limiting growth conditions—climatic limitations or tree-level water status—that allow or limit cambium activity and the formation of xylem cells (Eckes-Shephard et al., 2022; Körner, 2015). Although the mathematical description of these sink-limiting growth mechanisms of cells dates back to the 1960s (Lockhart, 1965), and attempts to model cambial activity followed shortly after (Wilson & Howard, 1968), their wider inclusion in mechanistic models of tree growth took place recently and remains scarce (De Schepper & Steppe, 2010; Holtta et al., 2010; Peters et al., 2021a; Steppe et al., 2006a; Steppe et al., 2008). Additionally, the role of turgor limitation in driving the growth of tropical trees has remained largely unexplored.

Recent global warming has increased the vapour pressure deficit (D; Grossiord et al., 2020), especially in the Neo-tropics (Barkhordarian et al., 2019), and South-East Asia (Deb et al., 2018). This increasing D has been shown to enhance the climate sensitivity of growth in temperate and boreal forests (Babst et al., 2018; Babst et al., 2019; Tumajer et al., 2022). For tropical moist forests, some source-driven global dynamic vegetation models predict continued increase in carbon sequestration during the next decades, in spite of increased temperature and—hence—D (Huntingford et al., 2013; Mercado et al., 2018). However, multiple studies found evidence for significant negative effects of drought (i.e., climatic water deficit) on tropical forest productivity (Doughty et al., 2015; Hubau et al., 2020; Liu et al., 2020; Phillips et al., 2009), often co-occurring with the impact of increasing D (Yuan et al., 2019), which is in line with findings from extra-tropical forest ecosystems (Babst et al., 2019). For example, a recent pan-tropical tree-ring study by Zuidema et al. (2022) highlights the importance of drought as stem growth positively responded to precipitation. Yet, whether the sole impact of increasing D on growth patterns in the tropics acts through source- or sink-limitation remains poorly quantified (Guan et al., 2015; Schippers et al., 2015a; Wagner et al., 2016).

Carbon-sink limitation occurs when the allocation of assimilated or stored carbon into plant biomass (e.g., roots, stems, branches, and leaves) is constrained by the environment. Sink-limited growth conditions for stem wood can, for example, be defined as environmental conditions under which secondary cambium cell division, expansion and cell wall thickening is impaired (Cuny et al., 2015; Cuny et al., 2019; Rathgeber et al., 2016; Steppe et al., 2015). Multiple processes, facilitating these wood formation processes, are directly affected by environmental conditions (Fatichi et al., 2014), including temperature-dependent cell wall extensibility (Parent et al., 2010) and changing water availability in the growing tissue impacting turgidity (Lockhart, 1965; Muller et al., 2011). Turgor can rapidly decrease with increasing D and decreasing soil water availability (Cabon et al., 2020; Peters et al., 2021a), yet due to methodological limitations, we mainly measure turgor-loss points in leaves (Bartlett et al., 2012; but see Bartlett et al., 2022 for root measurements), or osmolality in tree stems (a critical component of total turgor pressure; De Schepper & Steppe, 2010; Lintunen et al., 2016; Lazzarin et al., 2019). Additionally, although the onset of turgor-limitation can be inferred when high-resolution point dendrometer measurements records stem shrinkage (Zweifel et al., 2016), extracting the duration and absolute magnitude of turgor limitation using dendrometers is nontrivial. Therefore, we rely on mechanistic models to simulate in situ turgor pressure within the cambium (ψ_s^p; Cosgrove, 1986; Génard et al., 2001; Steppe et al., 2006a), by simulating the water flow and water potential (ψ) from the roots and the stem, to the canopy. Yet, mechanistic modelling of turgor-limited growth conditions is a 'data-hungry' practice (but see Potkay et al., 2022), and determining the environmental conditions under which it is limiting requires intra-annual and highly resolved information (e.g., Babst et al., 2021; Etzold et al., 2022). Such models need (sub)hourly dendrometer and sap flow data, providing data on night-time stem swelling and day-time shrinkage dynamics (Salomón et al., 2022; Steppe et al., 2015; Zweifel et al., 2021), which are sparse in tropical forests (but see De Mil et al., 2019; Eller et al., 2018; Kaewmano et al., 2022).

Tree-internal water fluxes, which steer turgor variability in growing tissue, are largely regulated by stomatal control (Potkay & Feng, 2023; see also Dewar et al., 2022; Peters et al., 2023). Stomatal closure is a key mechanism for trees to balance the fixation of atmospheric CO_2 with the loss of water (Buckley, 2019; Edwards et al., 1998). High D induces water loss via leaf transpiration and causes an increase in tension of the water column, commonly quantified by more negative leaf water potential measurements (ψ_{leaf}). More negative ψ_{leaf} relates well to the closure of stomata (Anderegg et al., 2017; Buckley et al., 2003), where tropical species appear to reduce their stomatal conductance to 50% at a ψ_{leaf} of around −1.5 MPa (Klein, 2014), although its variance is highly species-specific (e.g., Flo et al., 2021; Johnson et al., 2009; Martínez-Vilalta & Garcia-Forner, 2016; Medina-Vega et al., 2022; Meinzer et al., 1997; Wu et al., 2020). This threshold for stomatal closure is often assumed to optimise carbon assimilation against the threat of significant xylem conductance loss (Brodribb et al., 2017; Joshi et al., 2022; Wang et al., 2020; Wolf et al., 2016), a process occurring well beyond ψ_{leaf} conditions that limit turgor build-up for growth (e.g., Muller et al., 2011). We thus expect at the daily to seasonal scale that turgor-limitation of growth conditions is aggravated when stomata have not yet fully closed, in addition to the turgor limitation imposed by periods of low soil water availability (see Peters et al., 2021a). If this would be the case, it is an indication that cambial turgidity (i.e., the sink) constrains intra-annual growth rate in addition to photosynthetic activity (i.e., the source).

In this study, we apply a turgor-driven mechanistic model, that was tested for conifer trees in high-elevation temperate forests (Peters et al., 2021a), to quantify the environmental conditions causing turgor to limit intra-annual stem diameter growth rates in a

widely distributed tropical tree species *Toona ciliata* M. Roem. We used a unique set of wood formation observations, and high-resolution point dendrometer (see Kaewmano et al., 2022) and sap flow data measured on five mature *T. ciliata* trees growing in an Asian tropical rainforest in Southern China. In addition, we measured bi-weekly pre-dawn and midday leaf water potential dynamics (ψ_{leaf}) and modelled stomatal conductance behaviour with the sap flow measurements to assess stomatal control dynamics to increasing D. We hypothesise that: (1) diel growth dynamics in *T. ciliata* are congruent with turgor pressure dynamics, with growth mainly occurring at night (Steppe et al., 2015; Zweifel et al., 2021), (2) variability in intra-annual growth dynamics is largely explained by changing turgor pressure dynamics (Steppe et al., 2006a), and (3) tropical trees experiencing high D, during high midday temperatures, are assumed to face stronger turgor-limited radial stem growth as stomatal control prioritises carbon assimilation and solely prevent water loss which causes embolisms (e.g., safety-efficiency modelling paradigm; Joshi et al., 2022) instead of the thresholds at which turgidity is lost.

2 | MATERIALS AND METHODS

2.1 | Site description and study design

To test our hypotheses, we conducted continuous monitoring for 1 year in a tropical rainforest near the Xishuangbanna Tropical Botanical Garden, Yunnan province in southwest China (Figure 1). This forest is a tropical seasonal rainforest on acid soils with clay-loamy texture (21.58°N, 101.09°E, 922 m a.s.l.). This site was selected for its distinct seasonal variability in vapour pressure deficit (D; Figure 1a), and lower variability in soil water potential (ψ_{soil}; Figure 1b). The climate of the research region is influenced by warm and wet air masses from the Indian Ocean during summer and continental cold and dry air masses in winter. As such, the rainy season occurs from May to October and the dry season from November to April (Cao et al., 2006). The long-term (1959–2017) mean annual temperature is 21.9°C, with an annual maximum temperature of 29.7°C, and a mean annual precipitation of 1473 mm (as described in Kaewmano et al., 2022).

At the site, five dominant *Toona ciliata* M. Roem. trees were selected for continuous monitoring, on which we measured a plethora of allometric properties (Table 1). The mean height (h_{tree}) of the selected trees was 18.8 ± 3.3 m, with an average diameter at breast height (1.3 m above the ground; *DBH*) of 28.3 ± 8.2 cm, and a mean sapwood thickness (t_{sw}) of 3.21 ± 0.5 cm (measured by detecting translucence differences on two fresh wood cores taken at breast height by using an increment borer; Haglöf, Sweden). Individuals of *T. ciliata* were leafless during late October and November for about 1 month, and flushed new leaves during the dry foggy season from December to January. Maximum canopy cover was found from May to September (Kaewmano et al., 2022).

2.2 | Continuous high-resolution monitoring

Environmental measurements covered the entire physiological monitoring period from January to December 2019. Air temperature (T_a, in °C), relative humidity (%), solar irradiance (W m^{-2}), and precipitation (mm) were monitored at the Xishuangbanna Tropical Botanical Garden (21.54°N, 101.46°E, 580 m a.s.l.) at 10-min intervals. Relative humidity and T_a were used to calculate D (kPa) using the 'plantecophys' R package (Duursma, 2015; according to Jones, 2013). Additionally, ψ_{soil} (MPa) was derived by using pedo-transfer functions, which are based on parameters presented in Teepe et al. (2003) and the soil texture and bulk density described in Kaewmano et al. (2022), on locally measured soil water content at a soil depth of 20, 40 and 60 cm. The resulting ψ_{soil} dynamics were validated against pre-dawn leaf water potential (ψ_{leaf}) dynamics (Supporting Information: Figure S1). All monitoring data was inspected for outliers by using the datacleanr R package (Hurley et al., 2022) in the R software (version 4.0.2; R Core Team, 2017).

For all five trees in Table 1, we monitored over-bark stem diameter variations (Δd_{stem}, in µm) using automated point dendrometers (DRW type, Ecomatik). These dendrometers were installed at ca. 1.3 m above the ground on the stem and recorded Δd_{stem} every 10 min. To minimise the effect of hygroscopic expansion and
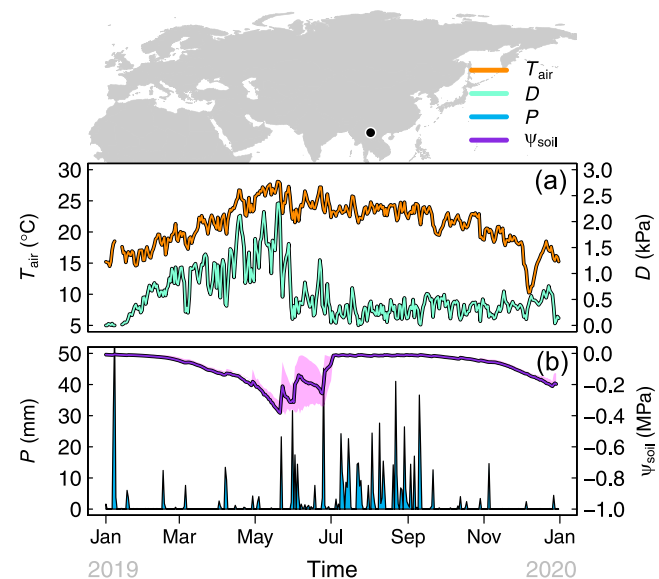
FIGURE 1 Climatic conditions during the 2019 monitoring period at the Xishuangbanna Tropical Botanical Garden, Yunnan province in southwest China. (a) Daily mean atmospheric temperature (T_{air}) and vapour pressure deficit (D) measured in Xishuangbanna Tropical Botanical Garden (21.54°N, 101.46°E, 580 m a.s.l.). (b) Daily precipitation dynamics measured at the Xishuangbanna Tropical Botanical Garden and modelled soil water potential (ψ_{soil}) using local measurements of average volumetric soil water content at 20, 40 and 60 cm depth (with the range measured at different depths indicated in pink). The black dot in the map indicates the study site.

TABLE 1 Characteristics of trees instrumented for continuous monitoring and relevant for model parameterisation.

Species	Plant functional type	Tree code	DBH (cm)	h_{tree} (m)	h_{stem} (m)	t_{sw} (cm)	t_{ba} (cm)	t_{phl} (cm)	Δd_{stem} (cm)	$F_{crown\ max}$ (g h^{-1})
Toona ciliata	Semi diffuse-porous	T1	42.7	15.0	10.3	2.85	1.25	0.80	2.35	3779
		T2	32.3	20.2	12.2	2.75	0.99	0.89	1.46	1438
	Deciduous	T8	22.3	22.0	13.0	3.75	0.77	0.58	2.77	2298
	Broad-leaved	T9	22.5	22.1	15.1	2.95	0.69	0.50	2.58	1859
		T11	21.5	14.7	8.7	3.75	0.89	0.65	1.71	1844

Note: For each individual tree, diameter at breast height (*DBH*), tree height (h_{tree}), stem length (h_{stem}), sapwood thickness (t_{sw}), maximum bark thickness (t_{ba}) and phloem thickness (t_{phl}) were measured. Additionally, the annual increment for the stem diameter of 2019, derived from the dendrometer (Δd_{stem}), and the maximum sap flow ($F_{crown\ max}$), derived from sap flow sensors, are provided for the year 2019.

shrinkage, the outermost dead layer of the bark was removed. The raw dendrometer data of each tree were processed using the 'treenetproc' R package (Knüsel et al., 2021). The final d_{stem} (required for model calibration) was calculated from the Δd_{stem} measurements and tree diameter (i.e., *DBH*), considering only xylem and phloem ([Δd_{stem} + DBH] – t_{ba} × 2 + t_{phl} × 2; see Table 1).

To quantify sap flow dynamics, we equipped the study trees with homemade thermal dissipation probes (according to Granier 1985; see also Lu et al., 2004), installed at 1.3 m height on the northeast side of a stem. Two 20 mm long probes were radially inserted into the xylem (below the cambium), with a vertical distance of 10 cm and shielded from direct sunlight. The temperature difference between heated and unheated probe (ΔT, in °C) was recorded every 10 minutes with a sensor node (CR1000, Campbell). The ΔT measurements were processed into sap flux density (F_d, in kg m^{-2} s^{-1}) using the 'TREX' R package (Peters et al., 2021b), while considering (i) the double-regression method to establish zero-flow conditions (using a 5-day period), (ii) performing sapwood corrections (using t_{sw}), and (iii) wood-specific (diffuse-porous) calibrations (as calibration studies were not present for this semi diffuse-porous species). F_d was multiplied by sapwood area to obtain water flow to the crown (F_{crown}, in g h^{-1}).

2.3 | Leaf water potential measurements

Due to the destructive nature of leaf sampling for conducting leaf water potential measurements (ψ_{leaf}), five trees growing nearby the sampling trees were considered. From reachable branches, leaves were sampled pre-dawn (05:00, local time = UTC + 8) and midday (13:00) throughout the growing season. The sampling was performed on: 21/02/2019, 12/03/2019, 24/04/2019, 15/05/2019, 21/06/2019, 24/07/2019, 19/08/2019, 23/09/2019, 12/10/2019 and 13/11/2019. Directly after sampling, ψ_{leaf} was measured using a Scholander pressure bomb (Model 1000, PMS Instruments). These measurements aided in both elucidating stomatal behaviour to drought stress and supported model calibration.

2.4 | Stomatal behaviour analyses

The behaviour of canopy conductance (G_c) to drought stress was tested by analysing the species-specific response of G_c to *D*. We assessed the isohydricity (i.e., strictness of stomatal closure; Feng et al., 2018) by analysing the response of midday ψ_{leaf} to pre-dawn ψ_{leaf} and its linear relationship as proposed by Martínez-Vilalta et al. (2014). Furthermore, we calculated whole-tree canopy conductance (G_c, in mol m^{-2} s^{-1}) according to Flo et al. (2021; based on Phillips & Oren, 1998) from sap flow measurements to represent the mean stomatal behaviour of the entire tree crown. For each tree, we used the mean sap flow data between 10:00 and 15:00, corresponding to the hours with the highest radiation (i.e., peak-day data; Pappas et al., 2018), to calculate peak-day G_c values, as this limited time-window reduces the impact of stem capacitance and delayed flow dynamics (see Peters et al., 2019). Thus, peak-day F_d (in kg m^{-2} s^{-1}), *D* and T_a were used in Equation (1),

$$G_c = \frac{(115.8 + 0.4236 T_a)}{D} \frac{F_d}{\cdot} \eta \cdot \frac{T_0}{(T_0 + T_a)} \cdot e^{-0.00012 \cdot h} \quad (1)$$

where η is equal to 44.6 mol m^{-3}, T_0 is 273K and *h* (m) is the elevation of the site. Here, the terms (115.8 + 0.4236 T_a) are included to represent the temperature dependence of the conductance coefficient (see the term K_g in kPa m^3 kg^{-1} described in Phillips & Oren, 1998). The terms after and including η in Equation (1) represent unit transformations, converting conductance from m^3 m^{-2} s^{-1} to mol m^{-2} s^{-1} while accounting for the atmospheric pressure. Peak-day G_c values were removed where *D* < 0.3 kPa, as low *D* values cause inaccurate determinations of G_c, and when mean daily precipitation > 1 mm, as wet leaves distort the impact of *D* on stomatal conductance. As no information was available on the total leaf area and allometric equations seemed inadequate in reconstructing total leaf area, we standardised peak-day potential G_c expressed per unit of sapwood area to the maximum peak-day G_c per tree (G_c max as the 99th percentile of G_c; in accordance with Anderegg et al., 2017). Here we assume that no substantial changes in total leaf area occur during the analysis period, which we therefore confined to the period between full leaf expansion and before initial leaf loss. The response of standardised peak-day G_c to midday ψ_{leaf} and *D* was tested to infer about the points of stomatal closure due to drought.

2.5 | Turgor-driven growth model description

The continuous physiological monitoring and sampling were used to feed a mechanistic model, which extracted turgor-dynamics on a sub-daily scale and was used to test which environmental variables are limiting the sink-dynamics (see hypotheses 2 and 3). The mechanistic model consists of a water transport and stem diameter module, as detailed in Peters et al. (2021a; presented in Figure 2). The model presented by Peters et al. (2021a) based its mechanistic links between water fluxes and diameter variations on the general principles introduced by Steppe et al. (2006a). It uses similar structural components of the stem compartments (e.g., heart-wood and sapwood) and internal water relations (e.g., osmotic potential inference) as in the model explained in De Schepper & Steppe (2010), but excluding sugar loading dynamics. The model uses

tree-specific allometric characteristics, dendrometer and sap flow measurements and ψ_{soil}, to disentangle daily elastic shrinkage and swelling due to water transport from plastic volumetric wood formation (cell division and expansion), driving stem diameter growth.

In short, the turgor-driven growth model simulates water exchange between stem compartments induced by sap flow, which allows the assessment of differences in water potentials between compartments. The model considers three compartments, including the roots, stem and crown. The stem is modelled by three coaxial cylinders, including heartwood, water-conducting sapwood and an elastic stem storage compartment (consisting of cambium and phloem tissue). Water transport from the roots through the sapwood (F_{stem}, in $g\ h^{-1}$) is determined by the difference between root water potential (ψ_{root}, in MPa) and stem water potential (ψ_{stem}, in MPa) divided by the hydraulic resistance of the xylem (R_x, in MPa h g^{-1}; see Table 2).
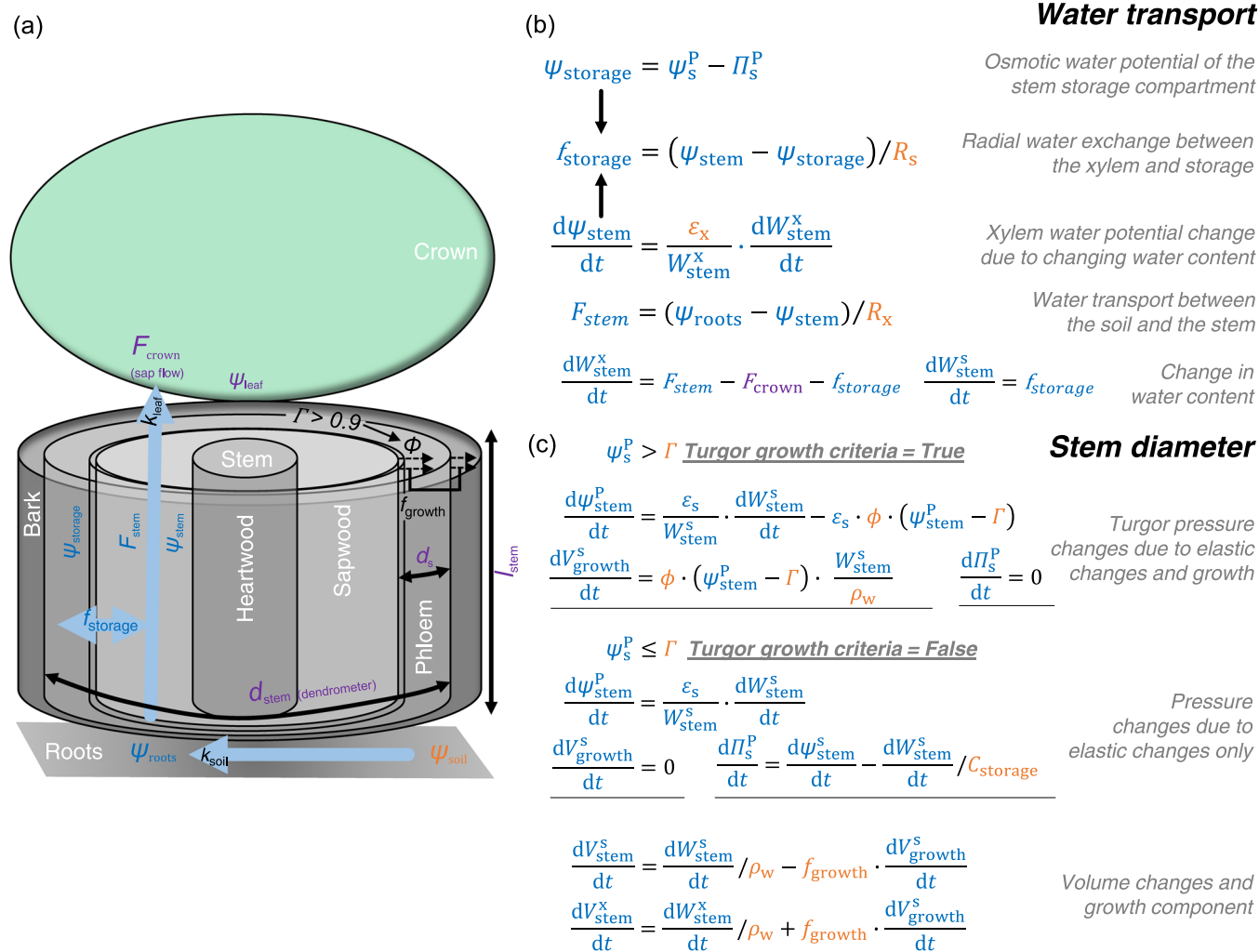
FIGURE 2 Water transport and stem diameter model used in the study (Peters et al., 2021a). (a) Graphical representation of the stem, with four stem tissues (heartwood, sapwood, phloem and bark). Colours indicate derived variables (in blue), parameters (in orange) or physiological/environmental measurements (in purple, see Table 2). (b) Equations describing the water transport model, from soil to atmosphere. Water flow is driven by transpiration (F_{crown}) and utilises either water moving from the soil (F_{stem}) or from the storage compartment ($f_{storage}$). (c) Equations describing the stem diameter model. Water transport and status drive diameter growth by impacting pressure ($\psi_{storage}$) and turgor (ψ_s^P) of the storage compartment which consequently changes the stem diameter (d_{stem}). [Color figure can be viewed at wileyonlinelibrary.com]

TABLE 2 Symbol, unit and description of the model parameters, monitoring data, algebraic variables and derived variables.

Type	Symbol	Unit	Description
Parameters	ρ_w	g m^{-3}	Density of water.
	l_{stem}	m	Length of the stem.
	d_{stem}^i	m	Initial diameter of the outer diameter of the stem segment (DBH).
	d_s	m	Initial thickness of the stem storage compartment.
	r_{hw}	m	Radius of the non-conductive xylem (heartwood).
	$C_{storage}$*	g MPa^{-1}	Capacitance of the stem storage compartment.
	R_x*	MPa h g^{-1}	Flow resistance in the stem compartment of the active xylem (sapwood).
	R_s*	MPa h g^{-1}	Exchange resistance between the active xylem of the stem and the storage compartment (bark).
	Π_s^i*	MPa	Initial osmotic pressure of living tissue of the stem.
	f_{water}	Unitless	Water fraction of the stem compartment.
	k_{leaf}	Unitless	Proportionality constant for calculating ψ_{stem} from $\psi_{leaf,}$ is set to 1.
	ε_0	m^{-1}	Elastic modulus (ε_s) is proportional (ε_0) to the product of the outer diameter and the pressure potential.
	ε_x	MPa	Elastic modulus of the xylem.
	Φ	MPa^{-1} h^{-1}	Extensibility of cell walls in relation to non-reversible dimensional changes (radial wood growth).
	Γ	MPa	Threshold turgor pressure.
	f_{growth}	Unitless	Fraction of growth contributing to xylem formation.
	ψ_{soil}^i	MPa	Initial soil water potential.
	k_{soil}	Unitless	Proportionality constant for calculating ψ_{roots}.
	t_{phloem}	cm	Thickness of the visually distinguishable phloem (assumed to equal d_s).
	t_{bark}	cm	Overall thickness of the bark of the stem.
	$t_{sapwood}$	cm	Thickness of the visually distinctive sapwood.
Monitoring data	F_{crown}	g h^{-1}	Water flow from the stem xylem towards the crown compartment (obtained from F_d).
	F_d	cm^3 m^{-2} h^{-1}	Measurement of sap flux density using thermal dissipation probes.
	d_{stem}	m	Over bark diameter (obtained from r_{stem}).
	r_{stem}	μm	Dendrometer measurement of the stem radius.
	r_{xyl}	μm	Radius of the xylem (obtained from xylogensis observations).
	ψ_{leaf}	MPa	Leaf water potential (measurements).
	ψ_{soil}	MPa	Soil water potential (measurements).
	R_g	W m^{-2}	Global radiation.
	RH	%	Relative air humidity.
	T_a	°C	Air temperature.

Type	Symbol	Unit	Description
Algebraic variables	f_{stem}	g h^{-1}	Water exchange between the xylem and the storage compartment.
	F_{stem}	g h^{-1}	Water flow from the roots towards the stem xylem compartment.
	d_{stem}^{x}	m	Xylem diameter of the stem segment.
	d_{stem}	m	Outer diameter of the stem.
	ε_s	MPa	Bulk elastic modulus of living tissue in relation to reversible dimensional changes.
	ψ_{roots}	MPa	Root water potential.
	$\psi_{storage}$	MPa	Water potential in the storage compartment.
	ψ_{stem}	MPa	Stem water potential.
	D	kPa	Vapour pressure deficit.
Derived variables	W_{stem}^{x}	g	Water content in the stem xylem compartment.
	W_{stem}^{s}	g	Water content in the stem storage compartment.
	ψ_{stem}	MPa	Pressure component of the xylem water potential.
	ψ_s^{P}	MPa	Pressure component of the water potential in the storage compartment.
	V_{stem}^{x}	m^3	Volume of the stem xylem tissue.
	V_{stem}^{s}	m^3	Volume of the stem storage compartment.
	V_{growth}^{s}	m^3	Growth volume for the entire stem.
	Π_s^{P}	MPa	Osmotic component of the water potential in the storage compartment.

Note: Symbols highlighted with * were considered for the mechanistic model calibration. See Figure 2 for a schematic representation of the applied model.

Moreover, the model simulates ψ_{leaf} which was used for model calibration (see detailed description of the calibration procedure below). Initial nighttime ψ_{leaf} values, required for initiating the simulation, were provided by adding the known decrease of −0.01 MPa m^{-1} tree height (Koch et al., 2004), due to the gravitational force, to the ψ_{soil} conditions. Here it was assumed that there was negligible nocturnal transpiration, that is, assuming complete stomatal closure, during the initial nighttime. The imbalance between F_{stem} and water transported to the crown (F_{crown}, in g h^{-1}) defined the amount of water that is used from the storage compartment ($f_{storage}$), and is calculated using the resistance for radial water transport between the xylem and phloem (R_s, in MPa h g^{-1}) and the capacitance of the tissue to release water ($C_{storage}$, in g MPa^{-1}). The model thus estimates the storage water potential ($\psi_{storage}$, in MPa) and, subsequently, the volume of water in the storage compartment (V_{stem}^{s}, in m^3). Depending on the osmotic potential (Π_s^{i}, in MPa), for which the initial value is fixed and changes depending upon the volumetric change of the storage tissue, these dynamics are used to determine turgor pressure in the storage compartment (ψ_s^{P}, in MPa). Daily reversible fluctuations in d_{stem} (as seen in dendrometer measurements) are determined by turgor changes in sapwood (affected by its elastic modulus; ε_x, in MPa) and storage compartment (determined by the elastic modulus of the

storage compartment; ε_s, in MPa; see De Schepper & Steppe, 2010). The dynamics of ψ_s^{P} are used to calculate irreversible stem diameter growth (d_{stem}^{x}). Growth occurs when ψ_s^{P} exceeds a threshold value for cell wall yielding (Γ, at 0.9 MPa; Lockhart, 1965; Steppe et al., 2006a; Table S1), which increases both the dimensions of the phloem and the xylem compartment (whose fractional investment is defined by f_{growth}). The increase in irreversible radial growth due to ψ_s^{P} exceeding Γ depends on the extensibility of cell walls (ϕ), which is a fixed parameter (Supporting Information: Table S1). To constrain the number of calibration parameters, and due to the fact that the temperatures are quite high (Figure 1), we did not consider the enzymatic dependence of ϕ as included in Peters et al. (2021a) to constrain growth at lower temperatures.

2.6 | Statistics and model calibration

We used the 'lme4' R package (Bates et al., 2015) to perform linear-mixed effect modelling for analysing the relation between turgor dynamics, growth, stomatal conductance and environmental conditions, including the tree as a random effect. For the daily analyses, we calculated pre-dawn (21:00 to 07:00) and midday (10:00 to

15:00) values for each of the dependent and independent variables. For each model fit, we carefully assessed model assumptions, including normality, heteroscedasticity and independence (Zuur et al., 2010). The significance of slopes and intercepts ($p < 0.05$) were obtained with the 'emmeans' R package (Lenth, 2022). The tree was added as a random intercept and a correction was included for the first-order autocorrelation detected in our residuals (applying an autocorrelation structure of order 1 in lme4). For the daily analyses of ψ_s^P dynamics and daily d_{stem}^x we solely consider days with data covering 24 h, thus excluding the initial day of a 5-day simulation. To explain the daily growth rate (Δd_{stem}^x), we adopted a logistic function to explain the response to D (Equation 2), where L is the maximum growth rate (set to maximum value detected with the dendrometer measurements, when correcting for bark growth with f_{growth} in Table 2), R is the minimum growth rate within the series, k is the logistic growth rate or steepness of the curve, and x_0 is the value of the sigmoid midpoint.

$$\Delta d_{stem}^x = \left(\frac{(L - R)}{1 + e^{-k(D - x_0)}} \right) + R. \tag{2}$$

Parameters for the turgor-driven growth model were established with existing literature and tree-specific measurements (see Supporting Information: Table S1). Model calibrations, simulations and sensitivity analyses were performed using the PhytoSim software (version 2.1, Plant AnalytiX) on each individual tree. Calibrations were performed for the measurements in 2019 for a total of 19 5-day periods when ψ_{leaf} was measured and accompanying time-series data (dendrometer and sap flow measurements) were available. These

calibrations were performed to analyse the behaviour of hydraulic parameters (R_x, $C_{storage}$, Π_s^i and R_s) and isolate turgor- and growth-dynamics. Due to data gaps and sensor errors, not all ψ_{leaf} dates were used for the model calibration procedure. Simulated xylem growth rates were validated according to Peters et al. (2021a) by using biweekly wood formation data collected and presented in Kaewmano et al. (2022) considering intra-annual stem diameter changes due to wood cell division and expansion.

3 | RESULTS

3.1 | Seasonal variability of input data and model validity

During the 2019 growing season, the five monitored trees showed an annual diameter growth of 2.17 ± 0.57 cm (Table 1). The seasonal dynamics revealed that the maximum weekly growth rate ($\Delta d_{stem\ weekly}$) was reduced in May and June, compared to the periods with maximum growth rates observed in April and the beginning of July (Figure 3a). The monthly specific diurnal patterns revealed that maximum stem swelling was obtained around 8:00, with the strongest maximum daily shrinkage patterns observed in the period from March until June (Figure 3b). Maximum stem shrinkage throughout the year was obtained around 17:00, with January and December showing the lowest daily shrinkage. The trees showed an absolute maximum transpiration rate of 2.2 ± 0.9 kg of water per hour (Table 1), with substantially reduced
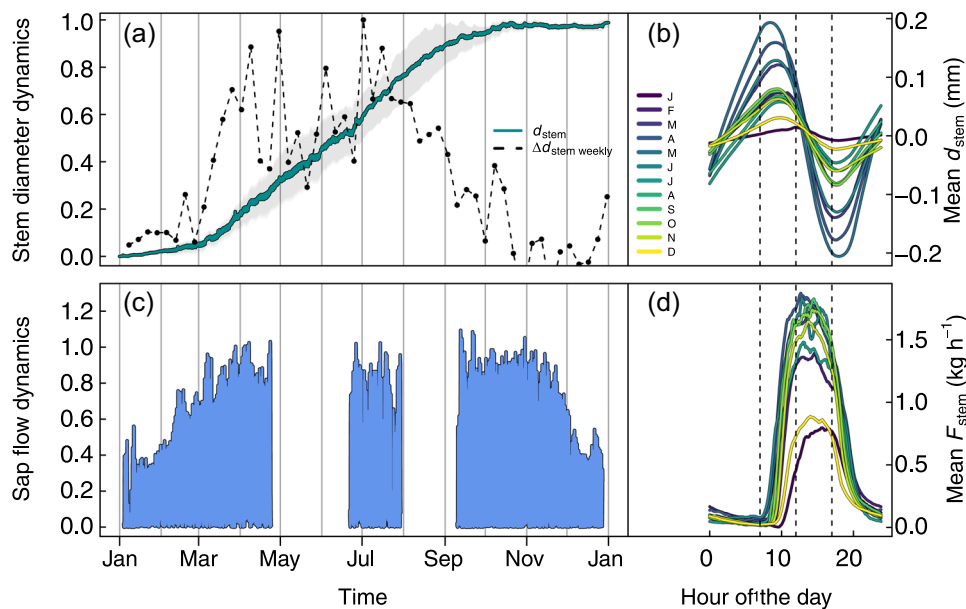

FIGURE 3 Stem diameter and sap flow dynamics of *Toona ciliata* trees in 2019. (a) Mean relative seasonal stem diameter (d_{stem}) development for five trees. Diameter measurements were scaled from 0 to 1. The shaded grey area is the 95% confidence interval of the measurements. The dots indicate the mean weekly growth rate of d_{stem}. (b) Mean monthly diurnal dynamics of delta-corrected d_{stem}, averaged per month. Dashed black lines indicate 07:00, 12:00 and 17:00, respectively. (c) Mean relative seasonal sap flow dynamics for five trees. Data were missing during part of the year. (d) Mean monthly diurnal patterns of water flow rate through the stem (F_{stem}). [Color figure can be viewed at wileyonlinelibrary.com]

transpiration rates in December, January and February (Figure 3c). Mean diurnal dynamics of sap water flow rate through the stem (F_{stem}) shows that maximum sap flow rates are obtained just past 12:00, with negligible sap flow occurring between 20:00 and 07:00 (Figure 3d).

The mechanistic model appeared to be effective in simulating stem diameter variations, where measured and simulated d_{stem} showed a clear linear relationship with an intercept approaching 0, and a residual mean squared error below 0.05 mm (Figure S2). Although the slope of the relation between measured and simulated d_{stem} approached 1, we found a slight overestimate of the simulated d_{stem} (slope = 0.88 ± 0.06). The mechanistic model revealed clear diurnal patterns in the sub-hourly dynamics of simulated leaf water potential (ψ_{leaf}), cell turgor pressure (ψ_s^P) and xylem diameter (d_{stem}^X) when calibrated on the dendrometer-derived d_{stem} measurements (M. in Figure 4). The 5-day simulations revealed a large variability in growth behaviour (concurrent with the growth observations), with the simulation around the beginning of March showing more nuanced growth mainly during the

night (Figure 4c), while those for July showed weaker turgor limitation, also at midday (Figure 4e).

3.2 | Diel turgor dynamics

The simulated turgor dynamics in the stem, obtained from the calibrated model during the growing season (Figure 4a), revealed distinct diel patterns as a function of D (Figure 5). Days with low midday D (0–0.5 kPa) show 24 h of growth, where ψ_s^P is above the turgor limitation threshold for allowing cell wall yielding (Γ = 0.9 MPa; Figure 5a). As soon as midday D crosses 0.5 kPa, higher daily mean D appears to limit turgor, with Γ being crossed around 11:00 (Figure 5b–d), while the time where $\psi_s^P > \Gamma$ (commonly at the end of the day) appears to depend upon the level of D_{midday}. This leads to a distinct pattern where the recovery of turgor pressure suitable for growth appears to occur later during the day, that is, 23:00 with 0.5–1 kPa D_{midday} and 01:00 with 1.5–2.5 kPa D_{midday} (see Figure 5b,d, respectively). Moreover, an increase in D_{midday} appears
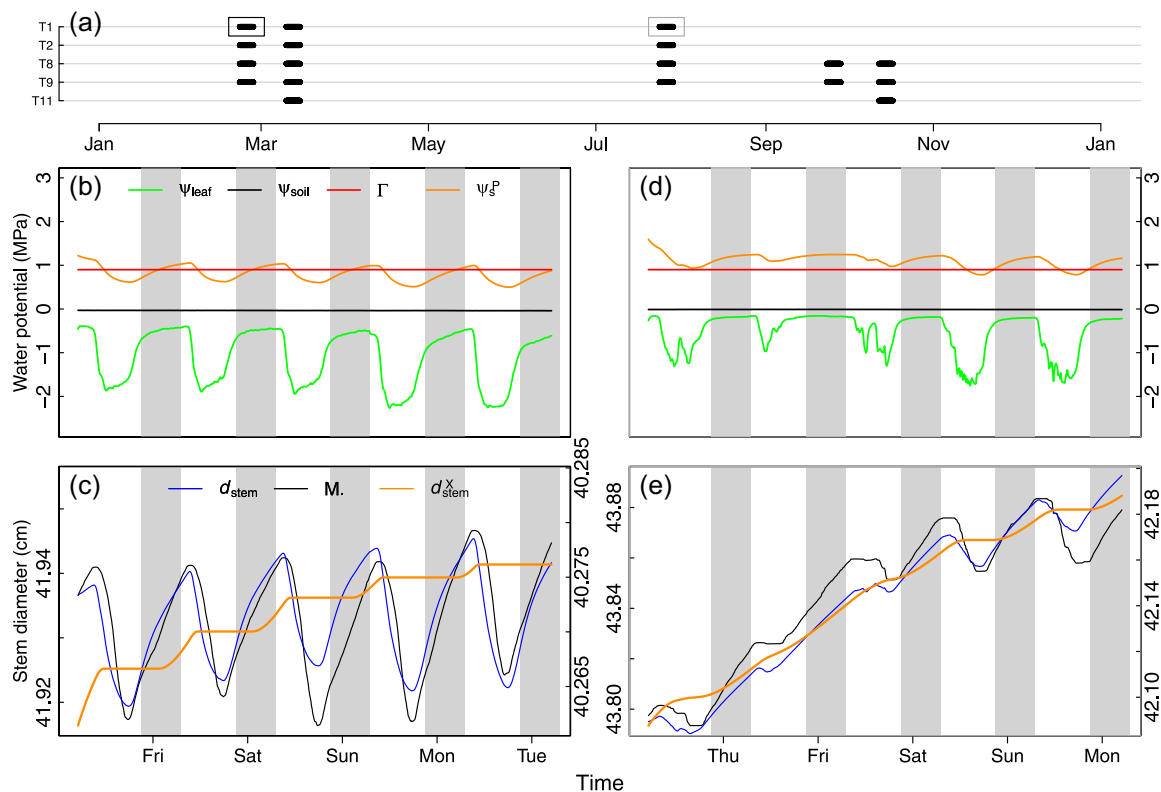

FIGURE 4 Simulated water potential and stem diameter dynamics carried out for the 5-day period simulations (a) and example of a simulation for tree T1 starting on the 21st of February 2019 (b, c; black rectangle in a), and the 24th of July 2019 (d, e; grey rectangle in a). Five days of simulated water potentials (b, d) and measured (M) diameter variations (c, e) for one of the *Toona ciliata* trees (T1; Table 1) during a growth period. Soil water potential (ψ_{soil}; b, d) and sap flow (F_{crown}) were used as model inputs, while leaf water potential (ψ_{leaf}; b) and simulated diameter variations (d_{stem}; left axis; c, e) were used for calibration. Growth of the xylem (d_{stem}^X; right axis; c) is predicted mainly for night-time hours, when cell turgor pressure (ψ_s^P; b) exceeds the critical value for wall-yielding (Γ). Grey-shaded areas indicate the times between 21:00 and 07:00, to highlight night-time periods. Each 5-day modelling period was based on a separate set of model parameters. [Color figure can be viewed at wileyonlinelibrary.com]
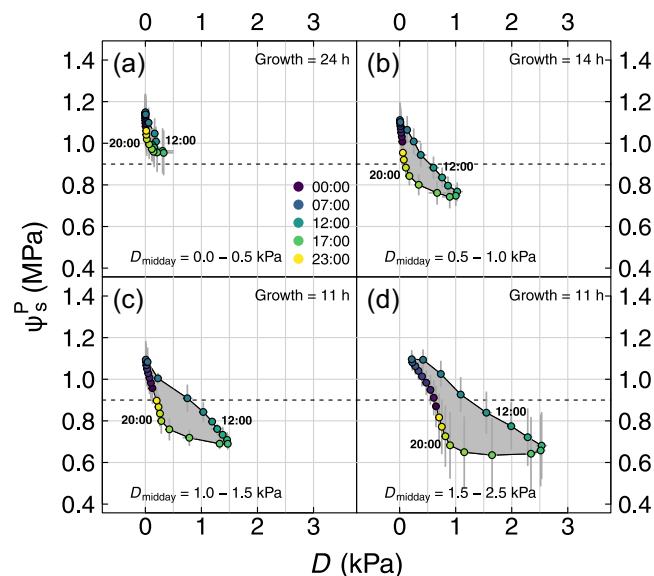
FIGURE 5 Diel impact of vapour pressure deficit (D) on turgor pressure in the cambium (ψ_s^P). Hourly averages of ψ_s^P and D are presented for days differing in current midday D (D_{midday}) conditions (a–d), based on mixed-effect models. Dots indicate the mean effect with 95% confidence interval. Colours reveal the specific hour of the day, with the response area highlighted with the grey shaded area. For each D_{midday}, growth hours are shown, that is, average number of hours with $\psi_s^P > 0.9$ MPa. [Color figure can be viewed at wileyonlinelibrary.com]

FIGURE 6 Previous midday vapour pressure deficit ($D_{previous\ midday}$) explaining pre-dawn turgor pressure in the cambium (ψ_s^P) and daily xylem growth (d_{stem}^x). (a) Relationship between $D_{previous\ midday}$ and pre-dawn ψ_s^P coloured by month. The solid line indicates the linear relationship with 95% confidence interval (dotted lines). (b) Logistic model of $D_{previous\ midday}$ and d_{stem}^x (Equation 2). The dashed line indicates highest observed stem growth from dendrometer measurements. (c) The simulated impact of the previous midday D ($D_{p.\ midday}$) on percentage d_{stem}^x using the relationship from (b) for the full growing season. [Color figure can be viewed at wileyonlinelibrary.com]

to severely reduce the hours in which growth is possible, with 11 h of growth as soon as D_{midday} crosses 1.0 kPa.

3.3 | Intra-annual turgor-driven growth dynamics

We found daily mean pre-dawn ψ_s^P (from 21:00 to 07:00) dynamics to be dependent on previous midday D (from 10:00 to 15:00). The linear mixed-effect modelling (considering the tree as a random intercept and correcting for first-order autocorrelation) revealed a significant linear relationship between D measured on the previous midday ($D_{previous\ midday}$) and pre-dawn ψ_s^P (slope = −0.12 MPa kPa^{-1}; $p < 0.001$), while current midday D did not significantly alter this relationship (slope = −0.03 MPa kPa^{-1}; $p = 0.096$). We therefore solely considered the $D_{previous\ midday}$ as a fixed effect (slope = −0.11 MPa kPa^{-1}; $p < 0.001$; Figure 6a) for further analyses. Moreover, although the relationship between mean pre-dawn ψ_{soil} and pre-dawn ψ_s^P was significant ($p = 0.001$; Supporting Information: Figure S3), when considering ψ_{soil} together with $D_{previous\ midday}$ to explain pre-dawn ψ_s^P no significant alteration of the slope was found ($p = 0.709$). The simulated daily xylem diameter growth (d_{stem}^x) showed a non-linear relationship, where we used Equation (2) to find a significant fit of R (37.6; $p < 0.0001$), k (−5.33; $p = 0.005$) and x_0 (0.16; $p = 0.007$). For this non-linear fit, L was considered as the 95th percentile of growth (215 µm d^{-1}), which was regarded as the point where 100% of the daily growth rate has been achieved (Figure 6b).
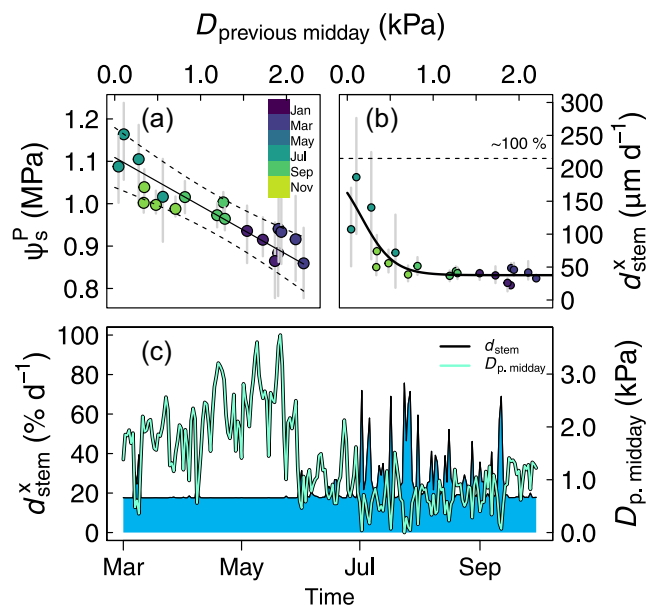
The fitted relationship revealed that daily xylem growth rates decreased until $D_{previous\ midday}$ reaches 1 kPa, after which they stabilised to a value of 38 µm d^{-1}. The fitted non-linear equation in Figure 6b was used to predict relative daily growth rate, which revealed higher growth rates after July (Figure 6c).

3.4 | Stomatal control and turgor-driven growth

Stomatal control extracted from the sap flow measurements revealed that canopy conductance (G_c) reached a plateau at 22% of the maximum (i.e., approaching stomatal closure), which relates to around 1.5 kPa of D (Supporting Information: Figure S4). When considering the plant water regulation of *T. ciliata*, we found that midday ψ_{leaf} dropped to strongly negative values compared to pre-dawn ψ_{leaf} (Figure 7a). Our linear mixed-effect model (including the tree as a random intercept and log$_{10}$ transformed independent variable which is back-transformed) showed no significant difference with the ψ_{leaf} values obtained from the model simulations (pre-dawn $\psi_{leaf} > −0.75$ MPa for common overlap; $p_{intercept} = 0.370$ and $p_{slope} = 0.080$). We tested the response of G_c to the simulated midday ψ_{leaf} (log$_{10}$ transforming both independent and dependent variable due to normality issues, which were back-transformed in Figure 7b), finding a significant slope and intercept ($p < 0.0001$) with the ψ_{leaf} at which
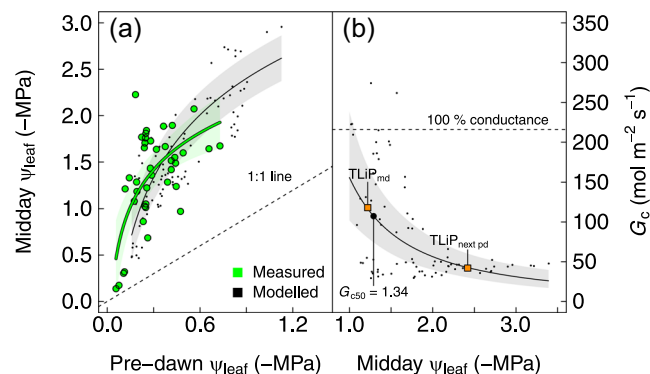
FIGURE 7 Tree water regulation determined by the relationship between pre-dawn and midday leaf water potential (ψ_{leaf}) and its relation to canopy conductance (G_c). (a) Comparison between the measured and modelled relationship between pre-dawn and midday ψ_{leaf}. For the simulated output, pre-dawn is considered as the average of ψ_{leaf} between 21:00 and 07:00, while midday covers 10:00 until 15:00. (b) The response of G_c to midday ψ_{leaf}, described by a $\log_{10}$ response of both the dependent and independent variable. The point where 50% of G_c (G_{c50}) is lost and the turgor limitation point for both midday (TLiP_{md}) and pre-dawn ($\mathrm{TLiP}_{next\ pd}$; or the following night TLiP) ψ_{leaf} conditions are provided (and further detailed in Supporting Information: Figure S5). Note that absolute values for ψ_{leaf} are used due to $\log_{10}$ transformation (which was back-transformed). The smaller black dots in both panels represent the raw measurements from the model. [Color figure can be viewed at wileyonlinelibrary.com]

50% of G_c is lost at −1.34 MPa (G_{c50}; Figure 7b). The approximated stomatal conductance plateau (i.e., 22% of $G_c/G_{c\ max}$; approaching stomatal closure) was reached at −2.25 MPa midday ψ_{leaf}. When considering pre-dawn and midday ψ_s^P, we found a strong linear relationship between previous midday ψ_{leaf} and pre-dawn ψ_s^P (Supporting Information: Figure S5a; $p < 0.001$). The point at which turgor limitation occurred for the following night (−2.42 MPa; Supporting Information: Figure S5a) is more negative than the point at which G_{c50} is reached, and is close to the ψ_{leaf} at which stomatal closure is reached (−2.25 MPa; Figure 7b). The relationship between current midday ψ_{leaf} also shows significant relationship with current midday ψ_s^P (Supporting Information: Figure S5b; $p < 0.001$), where G_{c50} matches the point at which the turgor limitation point is reached. Stomatal control appears particularly tuned to prevent reaching turgor-loss during the following day's pre-dawn conditions (i.e., G_c values reaching its minimum close to $\mathrm{TLiP}_{next\ pd}$), although we should note that G_c never appears to reach 0 mol m^{-2} s^{-1} in *T. ciliata* (Figure 7b).

4 | DISCUSSION

In this study, we explored how environmental conditions induce turgor-limitation in stem growth and, in turn, can explain diel and seasonal patterns in stem diameter growth in the widespread tropical tree species *Toona ciliata*. In our tree model, this sink-limitation is

induced by a lack of turgor pressure in the cambium required to initiate xylem cell production and propagate cell expansion (Steppe et al., 2006a). For *T. ciliata*, we found vapour pressure deficit (*D*) to play a key role in steering turgor-limiting growth conditions on both a diel basis and at the seasonal scale. Although growth reductions are often attributed to a reduction in photosynthetic activity in the tropical biomes (Hashimoto et al., 2019; Nemani et al., 2003) and in our study species (Schippers et al., 2015a, 2015b), our case study reveals that sink-limitation can well-explain stem growth variability on the intra-annual level.

4.1 | Diel and seasonal importance of turgor-driven growth

The turgor-driven growth model provided realistic stem diameter estimates (Figure 4; Supporting Information: Figure S2), and parameters (Supporting Information: Table S2), falling within the expected range obtained from the literature (Supporting Information: Table S1; see Peters et al., 2021a). So far, turgor-driven growth models have been successful in simulating turgor-driven growth in mountain, temperate, and mangrove trees (De Schepper & Steppe, 2010; Peters et al., 2021a; Potkay et al., 2022; Steppe et al., 2006a; Steppe et al., 2018). Here we show that they also yield realistic output for mature tropical trees (Figure 4). On a diel basis, we confirm the findings by Zweifel et al. (2021) for a tropical tree species: growth of our study species primarily occurs at night (Steppe et al., 2015; supporting our first hypothesis). We show that in the rare case when midday *D* conditions are exceptionally low (e.g., 0–0.5 kPa in Figure 5), growth can also occur during the day. After 11:00 AM, turgor pressure generally limited growth ($\psi_s^P < 0.9$ MPa; Génard et al., 2001). As soon as midday *D* exceeded 0.5 kPa, the loss of water delays the rehydration and thus limits the time window allowing stem growth (i.e., Figure 5b–d). For example, the number of growth hours (i.e., with sufficiently high turgor) is reduced by 3 h—or 21%—when *D* exceeds 1 kPa (Figure 5). Our findings on the importance of tree hydraulics in explaining sink limitation are in accordance with temperate trees, with particular relevance for night-time rehydration when experiencing drought stress (Salomón et al., 2022; Zweifel et al., 2007).

High midday *D* conditions can slow down night-time turgor build-up required for radial stem growth occurring in the following pre-dawn period (Figure 6a). This mechanism explains the stem diameter dynamics observed with dendrometers (Figure 3), and is in line with independent xylogenesis observations performed for the same species and site on a seasonal time scale (Kaewmano et al., 2022), showing the simulated stagnation in cell production and expansion around May and June of 2019 (Supporting Information: Figure S6). The pattern of increased turgor pressure in July (Figure 6a), causing the stimulation of daily xylem diameter (d_{stem}^x) growth (i.e., cell production and elongation dynamics, while not considering cell wall thickening; Cuny et al., 2015) also clearly coincided with conditions of low vapour pressure deficit (*D*) (Figure 6b,c). The importance of *D* in reducing water loss and

increasing tree internal water potentials has also been found for other species in central southern subtropical China (e.g., Luo et al., 2016), supporting the potentially more common occurrence of current pre-dawn growth limitation due to turgor for other species.

Our modelling output largely supports the use of the zero-growth concept in analysing dendrometer data (Zweifel et al., 2021), which assumes that structural growth (i.e., cell division and expansion) can only occur when the flexible stem tissues are not shrinking (i.e., when no tree water deficit occurs; Steppe et al., 2018). However, from both the diel- and seasonal-model simulations, it appears that growth can occur under mild conditions of stem shrinkage, which can be modulated by changes in the osmotic potential and the threshold for cell expansion (Donnellan Barraclough et al., 2018; Peters et al., 2021a; Steppe et al., 2006b). For example, xylem tissue is able to shrink in some cases, while the bark is expanding due to osmotic dynamics (Lazzarin et al., 2019). Thus, besides the importance of D in hampering turgor build-up in the wood-forming tissue, the interaction between sink- and source-limitation might be more important than currently used in plant growth models (Körner, 2015), and dynamic global vegetation models (Babst et al., 2021; Zuidema et al., 2018).

4.2 | Stomatal control in relation to retaining turgor pressure for growth

Stomatal control balances the loss of water with carbon assimilation (Damour et al., 2010; Wang et al., 2020). *T. ciliata* growing under conditions with limited influence of soil drought in 2019 (e.g., little reduction in pre-dawn leaf water potential [ψ_{leaf}] with decreasing soil water potential [ψ_{soil}]; Supporting Information: Figure S1), showed less strict stomatal regulation to decreasing water potentials. In other words, canopy conductance (G_c) did not substantially drop with decreasing midday ψ_{leaf} (Supporting Information: Figure S5a), where 50% stomatal closure was only reached around the expected −1.5 MPa for tropical trees (Klein, 2014; −1.34 MPa in Supporting Information: Figure S5b). Moreover, a plateau of G_c was reached at a D of 1.5 kPa (Supporting Information: Figure S4) and a ψ_{leaf} of −2.25 MPa (Figure 7b), which appears to be approaching the point of stomatal closure. This behaviour of slow stomatal response to changes in D or ψ_{leaf} is more commonly found in species with hydraulically efficient ring-porous sapwood (i.e., high maximum hydraulic conductance) that have ample access to soil water (Carminati & Javaux, 2020), when for instance compared to species with denser wood structure (i.e., diffuse-porous wood; lower maximum sapwood hydraulic conductivity in Flo et al., 2021). The finding that stomates show such a slow response and initiate closure only at relatively high D conditions suggests a water-spending water-use strategy of semi-diffuse porous *T. ciliata* and its adjustment to relatively wet year-round conditions. The risk of this strategy is however that the species could show a high xylem embolism vulnerability, with tropical angiosperm species showing 50% xylem

conductivity loss when ψ_{xylem} reaches −1 to −3 MPa (Chen et al., 2021; Choat et al., 2018).

The ψ_{leaf} value at which 50% of G_c is reached (−1.34 MPa G_{c50} in Figure 7b) is close to the point when current midday turgor pressure is lost (i.e., at a ψ_{leaf} −1.22 MPa). Interestingly, stomata appear to mostly close at ψ_{leaf} levels where night-time rehydration is sufficient to allow for ample turgor to facilitate at least some growth in the following night, although the rate is severely reduced (Figure 7b). This is apparent from the fact that the ψ_{leaf} at which stomata are reaching the previously identified plateau (ψ_{leaf} = −2.25 MPa) is close to the point at which the following pre-dawn ψ_s^P (or the coming night-time) would be fully below the turgor threshold (ψ_{leaf} = −2.42 MPa in Figure 7b). This finding supports the theory postulated by Potkay and Feng (2023), that lower water availability within the tree, and subsequent decreasing turgor in the cambium, are driven by stomatal regulation (see also Buckley, 2023). This is in stark contrast to the theory postulated by Joshi et al. (2022), which brings together two earlier optimisation theories (Prentice et al., 2014; Wolf et al., 2016) of stomatal control with the goal to maximise the difference between photosynthetic net carbon assimilation and the costs associated with decreasing leaf water potential (ψ_{leaf}). In these cases, the cost is either associated with xylem embolism formation and/or nitrogen use affecting the maximum rate of electron transport for photosynthesis (see also Manzoni et al., 2011 for a model overview). However, stomatal conductance regulation appears to be too weak during midday when D is high, resulting in delayed water refilling time and thus in the reduction of growth hours and cell expansion rate (Figure 5). This likely also explains the strong dependency of growth on previous midday D conditions (Figure 6). We thus hypothesise that this long-lived pioneer species' stomatal control is largely controlled by turgor (see also Trifilò et al., 2023). Yet, our trees do show some periods during which there is an instantaneous prioritisation for assimilation over water conservation under high water availability and high D. However, these periods are likely not the norm and over long drought periods, this prioritisation is likely to disappear when the stomatal aperture is regulated dynamically rather than instantaneously (Potkay & Feng, 2023). Overall our result shows that short periods of increased D induce a clear sink limitation of stem growth (see also Krejza et al., 2022; Zweifel et al., 2021), and decouples periods of daytime assimilation from those of nighttime stem growth. This finding may have important implications for timing and rate of tree growth under predicted increases in D under global change (Deb et al., 2018; Grossiord et al., 2020).

If decoupling of stomatal control and stem growth is common during the full growing season and across the distributional area of our study species, this may help explain why *T. ciliata*—and perhaps other tropical tree species—did not accelerate stem growth under increasing CO_2 levels, in spite of increased water-use efficiency (Groenendijk et al., 2015; van der Sleen et al., 2015). Our findings motivate the consideration of sink limitation, and specifically turgor, in mechanistic tree growth models (i.e., Schippers et al., 2015a) and vegetation models (Fatichi et al., 2014). Merging source- and sink-limiting processes in a mechanistic modelling

framework would allow us to quantify their relative importance in the face of ongoing climate change and CO_2 rise. Here especially, osmotic adjustments should be considered in a more mechanistic manner (i.e., De Schepper & Steppe, 2010), as our current model fixed initial osmotic potential and did not consider active regulation, which did not show clear environmental tendencies (i.e., higher values during periods of high D; Supporting Information: Table S2). Moreover, particular potential lies in simplifying the presented and data-hungry mechanistic models (i.e., presented here) into a more generalisable form. These next-generation models would need to be supported by the currently rare combination of in situ carbon assimilation measurements (i.e., in situ carbon-source measurements), non-structural carbohydrate assessments and wood formation observations.

4.3 | Conclusion and future prospects

Our study showed that the mechanistic modelling of turgor dynamics in the cambium is an effective tool to simulate and understand diel and seasonal growth dynamics of a tropical tree species. In this species, turgor limitation is highly sensitive to changes in atmospheric drought, probably driven by poor stomatal control. As we solely focused on a site with limited soil drying, we expect the importance of turgor limitation on growth to be even more prevalent in drier areas with sunny and warm conditions (i.e., high D) prevailing during the dry season (Aguirre-Gutiérrez et al., 2019; Feng et al., 2013). We still consider absolute assimilation rates important, particularly in explaining the absolute growth rates of an individual tree, but, it still has to be explored whether predictions on inter-annual growth variability of tropical trees can be improved when considering both sink- and source-limiting growth processes. Moreover, it remains to be tested if the mechanisms of source- and sink-limitation apply to pioneer tree species in general, and differs in more shade-tolerant species of tropical forests. These developments will allow for better disentangling of the roles of source- and sink-limited growth mechanisms in controlling stem growth and will ultimately improve the generic validity of growth model predictions of the forest biomes within the global carbon cycle.

CONFLICT OF INTEREST STATEMENT

The authors declare no conflict of interest.

DATA AVAILABILITY STATEMENT

The data that support the findings of this study are available from the corresponding author upon reasonable request.

SUMMARY STATEMENT

Stem growth dynamics of tropical rainforest trees are rarely linked to transpiration, although this directly impacts turgor-driven growth. We found turgor to limit intra-annual stem growth in *Toona ciliata*. Turgor limitation was enhanced during periods of high vapour pressure deficit.

ORCID

Richard L. Peters https://orcid.org/0000-0002-7441-1297
Ze-Xin Fan http://orcid.org/0000-0003-4623-6783
Frank Sterck https://orcid.org/0000-0001-7559-6572
Kathy Steppe http://orcid.org/0000-0001-6252-0704
Pieter A. Zuidema https://orcid.org/0000-0001-8100-1168

REFERENCES

Aguirre-Gutiérrez, J., Oliveras, I., Rifai, S., Fauset, S., Adu-Bredu, S., Affum-Baffoe, K. et al. (2019) Drier tropical forests are susceptible to functional changes in response to a long-term drought. *Ecology Letters*, 22, 855–865.

Anderegg, W.R.L., Wolf, A., Arango-Velez, A., Choat, B., Chmura, D.J. & Jansen, S. et al. (2017) Plant water potential improves prediction of empirical stomatal models. *PLoS One*, 12, e0185481.

Babst, F., Bodesheim, P., Charney, N., Friend, A.D., Girardin, M.P., Klesse, S. et al. (2018) When tree rings go global: challenges and opportunities for retro- and prospective insight. *Quaternary Science Reviews*, 197, 1–20.

Babst, F., Bouriaud, O., Poulter, B., Trouet, V., Girardin, M.P. & Frank, D.C. (2019) Twentieth century redistribution in climatic drivers of global tree growth. *Science Advances*, 5, eaat4313.

Babst, F., Friend, A.D., Karamihalaki, M., Wei, J., von Arx, G., Papale, D. et al. (2021) Modeling ambitions outpace observations of forest carbon allocation. *Trends in Plant Science*, 26, 210–219.

Barkhordarian, A., Saatchi, S.S., Behrangi, A., Loikith, P.C. & Mechoso, C.R. (2019) A recent systematic increase in vapor pressure deficit over tropical South America. *Scientific Reports*, 9, 15331.

Bartlett, M.K., Scoffoni, C. & Sack, L. (2012) The determinants of leaf turgor loss point and prediction of drought tolerance of species and biomes: a global meta-analysis. *Ecology Letters*, 15, 393–405.

Bartlett, M.K., Sinclair, G., Fontanesi, G., Knipfer, T., Walker, M.A. & McElrone, A.J. (2022) Root pressure–volume curve traits capture rootstock drought tolerance. *Annals of Botany*, 129, 389–402.

Bates, D., Mächler, M., Bolker, B. & Walker, S. (2015) Fitting linear mixed-effects models using lme4. *Journal of Statistical Software*, 67, 1–48.

Bonan, G.B. (2008) Forests and climate change: forcings, feedbacks, and the climate benefits of forests. *Science*, 320, 1444–1449.

Brodribb, T.J., McAdam, S.A. & Carins Murphy, M.R. (2017) Xylem and stomata, coordinated through time and space. *Plant, Cell & Environment*, 40, 872–880.

Buckley, T.N. (2019) How do stomata respond to water status? *New Phytologist*, 224, 21–36.

Buckley, T.N. (2023) Is carbon, not water, the resource that limits stomatal opening? *New Phytologist*, 238, 457–460.

Buckley, T.N., Mott, K.A. & Farquhar, G.D. (2003) A hydromechanical and biochemical model of stomatal conductance. *Plant, Cell & Environment*, 26, 1767–1785.

Cabon, A., Fernández-de-Uña, L., Gea-Izquierdo, G., Meinzer, F.C., Woodruff, D.R., Martínez-Vilalta, J. et al. (2020) Water potential control of turgor-driven tracheid enlargement in Scots pine at its xeric distribution edge. *New Phytologist*, 225, 209–221.

Cao, M., Zou, X., Warren, M. & Zhu, H. (2006) Tropical forests of Xishuangbanna, China. *Biotropica*, 38, 306–309.

Carminati, A. & Javaux, M. (2020) Soil rather than xylem vulnerability controls stomatal response to drought. *Trends in Plant Science*, 25, 868–880.

Chen, Y.-J., Maenpuen, P., Zhang, Y.-J., Barai, K., Katabuchi, M., Gao, H. et al. (2021) Quantifying vulnerability to embolism in tropical trees and lianas using five methods: can discrepancies be explained by xylem structural traits? *New Phytologist*, 229, 805–819.

Choat, B., Brodribb, T.J., Brodersen, C.R., Duursma, R.A., López, R. & Medlyn, B.E. (2018) Triggers of tree mortality under drought. *Nature*, 558, 531–539.

Cosgrove, D. (1986) Biophysical control of plant cell growth. *Annual Review of Plant Physiology*, 37, 377–405.

Cuny, H.E., Rathgeber, C.B.K., Frank, D., Fonti, P., Mäkinen, H. Prislan, P. et al. (2015) Woody biomass production lags stem-girth increase by over one month in coniferous forests. *Nature Plants*, 1, 15160.

Cuny, H.E., Fonti, P., Rathgeber, C.B.K., von Arx, G., Peters, R.L. & Frank, D.C. (2019) Couplings in cell differentiation kinetics mitigate air temperature influence on conifer wood anatomy. *Plant, Cell & Environment*, 42, 1222–1232.

Damour, G., Simonneau, T., Cochard, H. & Urban, L. (2010) An overview of models of stomatal conductance at the leaf level. *Plant, Cell & Environment*, 33, 1419–1438.

De Mil, T., Hubau, W., Angoboy Ilondea, B., Rocha Vargas, M.A., Boeckx, P., Steppe, K. et al. (2019) Asynchronous leaf and cambial phenology in a tree species of the Congo Basin requires space-time conversion of wood traits. *Annals of Botany*, 124, 245–253.

De Schepper, V. & Steppe, K. (2010) Development and verification of a water and sugar transport model using measured stem diameter variations. *Journal of Experimental Botany*, 61, 2083–2099.

Deb, J.C., Phinn, S., Butt, N. & McAlpine, C.A. (2018) Climate change impacts on tropical forests: identifying risks for tropical Asia. *Journal of Tropical Forest Science*, 30, 182–194.

Dewar, R., Hölttä, T. & Salmon, Y. (2022) Exploring optimal stomatal control under alternative hypotheses for the regulation of plant sources and sinks. *New Phytologist*, 233, 639–654.

Donnellan Barraclough, A., Zweifel, R., Cusens, J. & Leuzinger, S. (2018) Daytime stem swelling and seasonal reversal in the peristaltic depletion of stored water along the stem of *Avicennia marina* (Forssk.) Vierh. *Tree Physiology*, 38, 965–978.

Doughty, C.E., Metcalfe, D.B., Girardin, C.A.J., Amézquita, F.F., Cabrera, D.G., Huasco, W.H. et al. (2015) Drought impact on forest carbon dynamics and fluxes in Amazonia. *Nature*, 519, 78–82.

Duursma, R.A. (2015) Plantecophys - An R package for analysing and modelling leaf gas exchange data. *PloS one*, 10, e0143346.

Eckes-Shephard, A.H., Ljungqvist, F.C., Drew, D.M., Rathgeber, C.B.K. & Friend, A.D. (2022) Wood formation modeling—a research review and future perspectives. *Frontiers in Plant Science*, 13, 13.

Edwards, D., Kerp, H. & Hass, H. (1998) Stomata in early land plants: an anatomical and ecophysiological approach. *Journal of Experimental Botany*, 49, 255–278.

Eller, C.B., de V Barros, F., Bittencourt, P.R.L., Rowland, L., Mencuccini, M. & Oliveira, R.S. (2018) Xylem hydraulic safety and construction costs determine tropical tree growth. *Plant, Cell & Environment*, 41, 548–562.

Etzold, S., Sterck, F., Bose, A.K., Braun, S., Buchmann, N., Eugster, W. et al. (2022) Number of growth days and not length of the growth period determines radial stem growth of temperate trees. *Ecology Letters*, 25, 427–439.

Fatichi, S., Leuzinger, S. & Körner, C. (2014) Moving beyond photosynthesis: from carbon source to sink-driven vegetation modeling. *New Phytologist*, 201, 1086–1095.

Fatichi, S., Pappas, C., Zscheischler, J. & Leuzinger, S. (2019) Modelling carbon sources and sinks in terrestrial vegetation. *New Phytologist*, 221, 652–668.

Feng, X., Porporato, A. & Rodriguez-Iturbe, I. (2013) Changes in rainfall seasonality in the tropics. *Nature Climate Change*, 3, 811–815.

Feng, X., Ackerly, D.D., Dawson, T.E., Manzoni, S., Skelton, R.P., Vico, G. et al. (2018) The ecohydrological context of drought and classification of plant responses. *Ecology Letters*, 21, 1723–1736.

Flo, V., Martínez-Vilalta, J., Mencuccini, M., Granda, V., Anderegg, W.R.L. & Poyatos, R. (2021) Climate and functional traits jointly mediate tree water-use strategies. *New Phytologist*, 231, 617–630.

Friedlingstein, P., Jones, M.W., O'Sullivan, M., Andrew, R.M., Hauck, J. & Peters, G.P. et al. (2019) Research collection: global carbon budget 2019, *Optimal parameter tuning of feedback controllers with application to biomolecular antithetic integral control*, 10, pp. 12–19.

Friend, A.D., Eckes-Shephard, A.H., Fonti, P., Rademacher, T.T., Rathgeber, C.B.K., Richardson, A.D. et al. (2019) On the need to consider wood formation processes in global vegetation models and a suggested approach. *Annals of Forest Science*, 76, 49.

Génard, M., Fishman, S., Vercambre, G., Huguet, J., Bussi, C., Besset, J. et al. (2001) A biophysical analysis of stem and root diameter variations in woody plants. *Plant Physiology*, 126, 188–202.

Granier, A. (1985) Une nouvelle méthode pour la mesure du flux de sève brute dans le tronc des arbres. *Annales des Sciences Forestières*, 42, 193–200.

Groenendijk, P., van der Sleen, P., Vlam, M., Bunyavejchewin, S., Bongers, F. & Zuidema, P.A. (2015) No evidence for consistent long-term growth stimulation of 13 tropical tree species: results from tree-ring analysis. *Global Change Biology*, 21, 3762–3776.

Grossiord, C., Buckley, T.N., Cernusak, L.A., Novick, K.A., Poulter, B., Siegwolf, R.T.W. et al. (2020) Plant responses to rising vapor pressure deficit. *New Phytologist*, 226, 1550–1566.

Guan, K., Pan, M., Li, H., Wolf, A., Wu, J., Medvigy, D. et al. (2015) Photosynthetic seasonality of global tropical forests constrained by hydroclimate. *Nature Geoscience*, 8, 284–289.

Hashimoto, H., Nemani, R., Bala, G., Cao, L., Michaelis, A., Ganguly, S. et al. (2019) Constraints to vegetation growth reduced by region-specific changes in seasonal climate. *Climate*, 7, 27.

Holtta, T., Makinen, H., Nojd, P., Makela, A. & Nikinmaa, E. (2010) A physiological model of softwood cambial growth. *Tree Physiology*, 30, 1235–1252.

Hubau, W., Lewis, S.L., Phillips, O.L., Affum-Baffoe, K., Beeckman, H., Cuní-Sanchez, A. et al. (2020) Asynchronous carbon sink saturation in African and Amazonian tropical forests. *Nature*, 579, 80–87.

Huntingford, C., Zelazowski, P., Galbraith, D., Mercado, L.M., Sitch, S., Fisher, R. et al. (2013) Simulated resilience of tropical rainforests to CO_2-induced climate change. *Nature Geoscience*, 6, 268–273.

Hurley, A.G., Peters, R.L., Pappas, C., Steger, D.N. & Heinrich, I. (2022) Addressing the need for interactive, efficient, and reproducible data processing in ecology with the datacleanr R package. *PLoS One*, 17, e0268426.

Johnson, D.M., Woodruff, D.R., McCulloh, K.A. & Meinzer, F.C. (2009) Leaf hydraulic conductance, measured in situ, declines and recovers daily: leaf hydraulics, water potential and stomatal conductance in four temperate and three tropical tree species. *Tree Physiology*, 29, 879–887.

Jones, H.G. (2013) *Plants and microclimate: a quantitative approach to environmental plant physiology*, 3rd ed. Cambridge: Cambridge University Press.

Joshi, J., Stocker, B.D., Hofhansl, F., Zhou, S., Dieckmann, U. & Prentice, I.C. (2022) Towards a unified theory of plant photosynthesis and hydraulics. *Nature Plants*, 8, 1304–1316.

Kaewmano, A., Fu, P.-L., Fan, Z.-X., Pumijumnong, N., Zuidema, P.A. & Bräuning, A. (2022) Climatic influences on intra-annual stem radial variations and xylem formation of *Toona ciliata* at two Asian tropical forest sites with contrasting soil water availability. *Agricultural and Forest Meteorology*, 318, 108906.

Klein, T. (2014) The variability of stomatal sensitivity to leaf water potential across tree species indicates a continuum between isohydric and anisohydric behaviours. *Functional Ecology*, 28, 1313–1320.

Klesse, S., Babst, F., Lienert, S., Spahni, R., Joos, F., Bouriaud, O. et al. (2018) A combined tree ring and vegetation model assessment of European forest growth sensitivity to interannual climate variability. *Global Biogeochemical Cycles*, 32, 1226–1240.

Knüsel, S., Peters, R.L., Haeni, M., Wilhelm, M. & Zweifel, R. (2021) Processing and extraction of seasonal tree physiological parameters from stem radius time series. *Forests*, 12, 765.

Koch, G.W., Sillett, S.C., Jennings, G.M. & Davis, S.D. (2004) The limits to tree height. *Nature*, 428, 851–854.

Körner, C. (2015) Paradigm shift in plant growth control. *Current Opinion in Plant Biology*, 25, 107–114.

Krejza, J., Haeni, M., Darenova, E., Foltýnová, L., Fajstavr, M., Jan Světlík, S.větlík et al. (2022) Disentangling carbon uptake and allocation in the stems of a spruce forest. *Environmental and Experimental Botany*, 196, 104787.

Lazzarin, M., Zweifel, R., Anten, N. & Sterck, F.J. (2019) Does phloem osmolality affect diurnal diameter changes of twigs but not of stems in Scots pine? *Tree Physiology*, 39, 275–283.

Lenth, R.V. (2022) emmeans: Estimated Marginal Means, aka Least-Squares Means. R package. https://CRAN.R-project.org/package=emmeans

Lintunen, A., Paljakka, T., Jyske, T., Peltoniemi, M., Sterck, F., von Arx, G. et al. (2016) Osmolality and non-structural carbohydrate composition in the secondary phloem of trees across a latitudinal gradient in Europe. *Frontiers in Plant Science*, 7, 726.

Liu, L., Gudmundsson, L., Hauser, M., Qin, D., Li, S. & Seneviratne, S.I. (2020) Soil moisture dominates dryness stress on ecosystem production globally. *Nature Communications*, 11, 4892.

Lockhart, J.A. (1965) An analysis of irreversible plant cell elongation. *Journal of Theoretical Biology*, 8, 264–275.

Lu, P., Urban, L. & Ping, Z. (2004) Granier's Thermal Dissipation Probre (TDP) method for measuring sap flow in trees: theory and practice. *Acta Botanica Sinica*, 46, 631–646.

Luo, Z., Guan, H., Zhang, X., Zhang, C., Liu, N. & Li, G. (2016) Responses of plant water use to a severe summer drought for two subtropical tree species in the central southern China. *Journal of Hydrology: Regional Studies*, 8, 1–9.

Manzoni, S., Vico, G., Katul, G., Fay, P.A., Polley, W., Palmroth, S. et al. (2011) Optimizing stomatal conductance for maximum carbon gain under water stress: a meta-analysis across plant functional types and climates. *Functional Ecology*, 25, 456–467.

Martínez-Vilalta, J. & Garcia-Forner, N. (2017) Water potential regulation, stomatal behaviour and hydraulic transport under drought: deconstructing the iso/anisohydric concept. *Plant, Cell & Environment*, 40, 962–976.

Martínez-Vilalta, J., Poyatos, R., Aguadé, D., Retana, J. & Mencuccini, M. (2014) A new look at water transport regulation in plants. *New Phytologist*, 204, 105–115.

Medina-Vega, J.A., Wright, S.J., Bongers, F., Schnitzer, S.A. & Sterck, F.J. (2022) Vegetative phenologies of lianas and trees in two Neotropical forests with contrasting rainfall regimes. *New Phytologist*, 235, 457–471.

Meinzer, F.C., Andrade, J.L., Goldstein, G., Holbrook, N.M., Cavelier, J. & Jackson, P. (1997) Control of transpiration from the upper canopy of a tropical forest: the role of stomatal, boundary layer and hydraulic architecture components. *Plant, Cell & Environment*, 20, 1242–1252.

Mercado, L.M., Medlyn, B.E., Huntingford, C., Oliver, R.J., Clark, D.B., Sitch, S. et al. (2018) Large sensitivity in land carbon storage due to geographical and temporal variation in the thermal response of photosynthetic capacity. *New Phytologist*, 218, 1462–1477.

Muller, B., Pantin, F., Génard, M., Turc, O., Freixes, S., Piques, M. et al. (2011) Water deficits uncouple growth from photosynthesis, increase C content, and modify the relationships between C and growth in sink organs. *Journal of Experimental Botany*, 62, 1715–1729.

Nemani, R.R., Keeling, C.D., Hashimoto, H., Jolly, W.M., Piper, S.C., Tucker, C.J. et al. (2003) Climate-driven increases in global terrestrial net primary production from 1982 to 1999. *Science*, 300, 1560–1563.

Pan, Y., Birdsey, R.A., Fang, J., Houghton, R., Kauppi, P.E., Kurz, W.A. et al. A large and persistent carbon sink in the world's forests. Science, 333, 988–993.

Pappas, C., Matheny, A.M., Baltzer, J.L., Barr, A.G., Black, T.A., Bohrer, G. et al. (2018) Boreal tree hydrodynamics: asynchronous, diverging, yet complementary. *Tree Physiology*, 38, 953–964.

Parent, B., Turc, O., Gibon, Y., Stitt, M. & Tardieu, F. (2010) Modelling temperature-compensated physiological rates, based on the co-ordination of responses to temperature of developmental processes. *Journal of Experimental Botany*, 61, 2057–2069.

Peters, R.L., Speich, M., Pappas, C., Kahmen, A., von Arx, G., Graf Pannatier, E. et al. (2019) Contrasting stomatal sensitivity to temperature and soil drought in mature alpine conifers. *Plant, Cell & Environment*, 42, 1674–1689.

Peters, R.L., Steppe, K., Cuny, H.E., De Pauw, D.J.W., Frank, D.C., Schaub, M. et al. (2021a) Turgor—a limiting factor for radial growth in mature conifers along an elevational gradient. *New Phytologist*, 229, 213–229.

Peters, R.L., Pappas, C., Hurley, A.G., Poyatos, R., Flo, V., Zweifel, R. et al. (2021b) Assimilate, process and analyse thermal dissipation sap flow data using the TREX r package. *Methods in Ecology and Evolution*, 12, 342–350.

Peters, R.L., Steppe, K., Pappas, C., Zweifel, R., Babst, F., Dietrich, L. et al. (2023) Daytime stomatal regulation in mature temperate trees prioritizes stem rehydration at night. *New Phytologist*, 239, 533–546. Available from: https://doi.org/10.1111/nph.18964

Phillips, N. & Oren, R. (1998) A comparison of daily representations of canopy conductance based on two conditional time-averaging methods and the dependence of daily conductance on environmental factors. *Annales des Sciences Forestières*, 55, 217–235.

Phillips, O.L., Higuchi, N., Vieira, S., Baker, T.R., Chao, K.-J. & Lewis, S.L. (2009) Changes in Amazonian forest biomass, dynamics, and composition, 1980–2002, *Amazonia and global change*. Geophysical Monograph Series, pp. 373–387.

Potkay, A. & Feng, X. (2023) Do stomata optimize turgor-driven growth? A new framework for integrating stomata response with whole-plant hydraulics and carbon balance. *New Phytologist*, 238, 506–528.

Potkay, A., Hölttä, T., Trugman, A.T. & Fan, Y. (2022) Turgor-limited predictions of tree growth, height and metabolic scaling over tree lifespans. *Tree Physiology*, 42, 229–252.

Prentice, I.C., Dong, N., Gleason, S.M., Maire, V. & Wright, I.J. (2014) Balancing the costs of carbon gain and water transport: testing a new theoretical framework for plant functional ecology. *Ecology Letters*, 17, 82–91.

R Core Team. (2017) *R: A language and environment for statistical computing*. https://www.R-project.org/

Rathgeber, C.B.K., Cuny, H.E. & Fonti, P. (2016) Biological basis of tree-ring formation: a crash course. *Frontiers in Plant Science*, 7, 1–7.

Salomón, R.L., Peters, R.L., Zweifel, R., Sass-Klaassen, U.G.W., Stegehuis, A.I., Smiljanic, M. et al. (2022) The 2018 European heatwave led to stem dehydration but not to consistent growth reductions in forests. *Nature Communications*, 13, 28.

Schippers, P., Sterck, F., Vlam, M. & Zuidema, P.A. (2015a) Tree growth variation in the tropical forest: understanding effects of temperature, rainfall and CO_2. *Global Change Biology*, 21, 2749–2761.

Schippers, P., Vlam, M., Zuidema, P.A. & Sterck, F. (2015b) Sapwood allocation in tropical trees: a test of hypotheses. *Functional Plant Biology*, 42, 697–709.

van der Sleen, P., Groenendijk, P., Vlam, M., Anten, N.P.R., Boom, A., Bongers, F. et al. (2015) No growth stimulation of tropical trees by 150 years of CO_2 fertilization but water-use efficiency increased. *Nature Geoscience*, 8, 24–28.

Steppe, K., De Pauw, D.J.W. & Lemeur, R. (2008) A step towards new irrigation scheduling strategies using plant-based measurements and mathematical modelling. *Irrigation Science*, 26, 505–517.

Steppe, K., Sterck, F. & Deslauriers, A. (2015) Diel growth dynamics in tree stems: linking anatomy and ecophysiology. *Trends in Plant Science*, 20, 335–343.

Steppe, K., De Pauw, D.J.W., Lemeur, R. & Vanrolleghem, P.A. (2006a) A mathematical model linking tree sap flow dynamics to daily stem diameter fluctuations and radial stem growth. *Tree Physiology*, 26, 257–273.

Steppe, K., Saveyn, A., Vermeulen, K. & Lemeur, R. (2006b) A comprehensive model for simulating stem diameter fluctuations and radial stem growth, *Acta horticulturae*. Leuven, Belgium: International Society for Horticultural Science, pp. 35–42.

Steppe, K., Vandegehuchte, M.W., Van de Wal, B.A.E., Hoste, P., Guyot, A., Lovelock, C.E. et al. (2018) Direct uptake of canopy rainwater causes turgor-driven growth spurts in the mangrove *Avicennia marina*. *Tree Physiology*, 38, 979–991.

Teepe, R., Dilling, H. & Beese, F. (2003) Estimating water retention curves of forest soils from soil texture and bulk density. *Journal of Plant Nutrition and Soil Science*, 166, 111–119.

Trifilò, P., Abate, E., Petruzzellis, F., Azzarà, M. & Nardini, A. (2023) Critical water contents at leaf, stem and root level leading to irreversible drought-induced damage in two woody and one herbaceous species. *Plant, Cell & Environment*, 46, 119–132.

Tumajer, J., Scharnweber, T., Smiljanic, M. & Wilmking, M. (2022) Limitation by vapour pressure deficit shapes different intra-annual growth patterns of diffuse- and ring-porous temperate broadleaves. *New Phytologist*, 233, 2429–2441.

Wagner, F.H., Hérault, B., Bonal, D., Stahl, C., Anderson, L.O., Baker, T.R. et al. (2016) Climate seasonality limits leaf carbon assimilation and wood productivity in tropical forests. *Biogeosciences*, 13, 2537–2562.

Wang, Y., Sperry, J.S., Anderegg, W.R.L., Venturas, M.D. & Trugman, A.T. (2020) A theoretical and empirical assessment of stomatal optimization modeling. *New Phytologist*, 227, 311–325.

Wilson, B.F. & Howard, R.A. (1968) A Computer model for cambial activity. *Forest Science*, 14, 77–90.

Wolf, A., Anderegg, W.R.L. & Pacala, S.W. (2016) Optimal stomatal behavior with competition for water and risk of hydraulic impairment. *Proceedings of the National Academy of Sciences of the United States of America*, 113, E7222–E7230.

Wu, J., Serbin, S.P., Ely, K.S., Wolfe, B.T., Dickman, L.T., Grossiord, C. et al. (2020) The response of stomatal conductance to seasonal drought in tropical forests. *Global Change Biology*, 26, 823–839.

Yuan, W., Zheng, Y., Piao, S., Ciais, P., Lombardozzi, D., Wang, Y. et al. (2019) Increased atmospheric vapor pressure deficit reduces global vegetation growth. *Science Advances*, 5, 1–13.

Zuidema, P.A., Poulter, B. & Frank, D.C. (2018) A wood biology agenda to support global vegetation modelling. *Trends in Plant Science*, 23, 1006–1015.

Zuidema, P.A., Babst, F., Groenendijk, P., Trouet, V., Abiyu, A., Acuña-Soto, R. et al. (2022) Tropical tree growth driven by dry-season climate variability. *Nature Geoscience*, 15, 269–276.

Zuur, A.F., Ieno, E.N. & Elphick, C.S. (2010) A protocol for data exploration to avoid common statistical problems. *Methods in Ecology and Evolution*, 1, 3–14.

Zweifel, R., Steppe, K. & Sterck, F.J. (2007) Stomatal regulation by microclimate and tree water relations: interpreting ecophysiological field data with a hydraulic plant model. *Journal of Experimental Botany*, 58, 2113–2131.

Zweifel, R., Haeni, M., Buchmann, N. & Eugster, W. (2016) Are trees able to grow in periods of stem shrinkage? *New Phytologist*, 211, 839–849.

Zweifel, R., Sterck, F., Braun, S., Buchmann, N., Eugster, W., Gessler, A. et al. (2021) Why trees grow at night. *New Phytologist*, 231, 2174–2185.

SUPPORTING INFORMATION

Additional supporting information can be found online in the Supporting Information section at the end of this article.